Examination of the statistical rate theory expression for liquid evaporation rates

G. Fang* and C. A. Ward†
Thermodynamics and Kinetics Laboratory, Department of Mechanical and Industrial Engineering, University of Toronto, 5 King's College Road, Toronto, Ontario, Canada M5S 3G8
(Received 9 March 1998)

Recent measurements of the temperature at the interface of an evaporating liquid have been found to be in conflict with the predictions of classical kinetic theory. Under 20 different experimental conditions for water evaporation, the temperature in the vapor at the interface was measured to be greater than that in the liquid at the interface and this relation between the interfacial temperatures is the opposite to that predicted from classical kinetic theory. When these same data were used to examine the statistical rate theory (SRT) expression for the liquid evaporation rate, almost complete agreement was found. This theoretical approach is based on the transition probability concept, as defined in quantum mechanics, a hypothesis that assumes the rate of exchange between the possible quantum mechanical states of an isolated system that are within the energy uncertainty has the same value, and the Boltzmann definition of entropy. To determine whether the SRT expression for the evaporation rate also describes the liquid-vapor phase transition for liquids other than water, two hydrocarbons have been examined. The agreement between the predictions from SRT and the measurements is equally as good. These results raise the question of whether a quantum mechanical description is essential to describe the condition existing at the interface of an evaporating liquid. [S1063-651X(98)10712-2]

PACS number(s): 68.10.Jy

I. INTRODUCTION

Statistical rate theory (SRT) [1] has recently been used to develop an expression for predicting the rate of liquid evaporation [2]. This theoretical approach is based on the transition probability concept, as defined in quantum mechanics, and uses the Boltzmann definition of entropy to relate the predictions to measurable thermodynamic properties. The result of applying this procedure was the development of a complete expression (in the sense that there were no fitting parameters) for the liquid evaporation flux. The expression is in terms of the temperature and pressure in each phase at the phase boundary and known molecular and material properties of the substance evaporating. To examine the expression, it was used to predict the conditions under which water evaporated at a particular rate [2]; these predictions were compared with the measurements of water evaporation at 20 different experimental conditions that had been reported in Refs. [3] and [4]. The agreement was excellent and it was concluded that there was no measured disagreement [2].

There were, however, questions regarding the data of Refs. [3] and [4]. In both cases, the measurements indicated that during steady-state evaporation of water, the temperature in the vapor at the interface was *greater* than that in the liquid at the interface. This measured temperature discontinuity is in the *opposite* direction and its magnitude much larger, up to 7.8 °C [3], than that predicted from solutions of several different models of the Boltzmann equation. These solutions were obtained from different boundary conditions [5]. Since the measurements and the theory both strongly disagree with the predictions of classical kinetic theory and only water had been examined experimentally, the question arose whether there could have been a fortuitous canceling of errors that resulted in the close agreement between the predictions and the measurements in the case of water.

To examine the expression for the evaporation rate under different circumstances, the evaporation of two hydrocarbons that consist of differently shaped molecules has been studied: octane and methylcyclohexane. The former has a ''straight chain'' structure with one methyl (CH_3) at each end and six methylenes (CH_2) in between and the latter is a spherically shaped molecule with one methyl at an outside corner. At the same temperature, the hydrocarbons are more volatile than water. This has the advantage of allowing higher evaporation rates to be studied, but the disadvantage of making the determination of the temperature at the interface in each phase more difficult. The temperature exactly at the interface cannot be measured. As in the case of water, the continuum energy equation is solved using the temperature measured at different positions in the liquid and in the vapor phases as the boundary conditions and the temperature at the interface is then calculated from the solution of the continuum energy equation. For the hydrocarbons in contrast with water, the convective effects in the liquid cannot be neglected and a numerical procedure must be used to determine the temperature at the interface in each phase.

We find in each of five experimental circumstances with each liquid that at the interface, the temperature in the vapor is greater than the temperature in the liquid. Once these temperatures have been determined, they are used in the SRT expression for the evaporation rate to predict the pressure in the vapor at which a particular evaporation rate is expected. This predicted pressure can then be critically compared with that measured when the liquid is evaporating at that rate.

*Present address: Trojan Technologies, Inc., 3020 Gore Road, London, Ontario, Canada N5V 4T7.
†Author to whom correspondence should be addressed. FAX: 416-978-7322. Electronic address: ward@mie.utoronto.ca

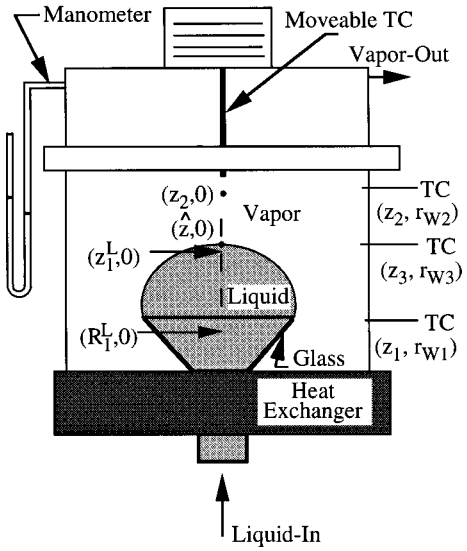

FIG. 1. Schematic diagram of the experimental apparatus. TC denotes thermocouple.

II. EXPERIMENTAL PROCEDURES

A schematic of the evaporation chamber used is shown in Fig. 1. The apparatus and experimental procedure is described in detail in Ref. [3]. Briefly, each liquid was pumped into the evaporation chamber at a constant rate with an infusion pump (0.5% accuracy over a liquid flow rate range 0.48–8.82 l/h). The liquid-vapor interface was visible from outside and the pressure in the chamber was adjusted until the liquid-vapor interface was observed with a cathetometer to be unmoving (accuracy ± 10 μm) for a period of 2 h. The temperature of each liquid entering the chamber was maintained at 26 °C with the heat exchanger indicated in Fig. 1.

Once a steady state had been reached, the temperature was measured with the three fixed thermocouples indicated in Fig. 1 and also on the center line at two positions in each phase with two differently sized thermocouples. With the small thermocouple (25.4-μm-diam wire) the temperature in the vapor was measured approximately 25 μm from the interface. When the temperature measurements were repeated approximately 1 h after they were first made, the maximum deviation in the temperature readings at any position was 0.5 K. The temperatures measured by the fixed thermocouples and by the movable thermocouple at two positions in each phase served as the boundary conditions for calculating the temperature field by the procedure described in Sec. III.

The liquids examined, octane (Aldrich®, 99+%, water less than 0.005%, evaporation residue less than 0.0003%) and methylcyclohexane (Aldrich®, 99+%, water less than 0.005%, evaporation residue less than 0.0005%), were degassed before they were used, but they were not otherwise purified. The conditions existing in the chamber were measured when each liquid was evaporating at one of five different rates. A summary of the experimental results is shown in Table I. The temperatures measured on the center line with the small thermocouple for the highest evaporation rate of each liquid are shown in Fig. 2.

Near the interface, the measured temperature in the vapor was higher than that in the liquid for all of the experiments with these hydrocarbons. This is consistent with the results obtained in the previous experiments with water. To determine the temperature at the interface, it is necessary to calculate the temperature profile.

III. INTERFACE AREA

To calculate the total energy flux into the liquid phase, the area of the interface is required. The interface is assumed axisymmetric and following the procedure developed in Ref. [4], the area may be predicted from the measured height of the interface on the center line a and the measured radius of the funnel at the point where the liquid-vapor interface intersects the funnel b. If the radius of curvature on the center line of the axisymmetric surface is denoted by R_c, then the coordinates of a point on the interface r_i, z_i may be expressed as a function of the turning angle ϕ [4],

$$dr_i = \frac{\cos\phi\, d\phi}{\frac{2}{R_c} + \left(\frac{\rho^L g}{\gamma^{LV}}\right)\left((a - z_i) - \frac{\sin\phi}{r_i}\right)} \tag{1}$$

and

$$dz_i = \frac{-\sin\phi\, d\phi}{\frac{2}{R_c} + \left(\frac{\rho^L g}{\gamma^{LV}}\right)\left((a - z_i) - \frac{\sin\phi}{r_i}\right)}, \tag{2}$$

with the boundary conditions

$$r_i(0) = 0 \tag{3}$$

and

$$z_i(0) = a, \tag{4}$$

where γ^{LV} is the surface tension, ρ^L the density of the liquid, and g the gravitational intensity. Equations (1) and (2) contain the unknown R_c. The independent variable of $r_i(\phi)$ and $z_i(\phi)$, ϕ, has a limited range

$$0 \leqslant \phi \leqslant \theta - \zeta, \tag{5}$$

where the contact angle is denoted as θ and the angle of the cone as ζ. At $\phi_{\max}$, $r_i(\phi)$ and $z_i(\phi)$ may be evaluated:

$$r_i(\theta - \zeta) = b \tag{6}$$

and

$$z_i(\theta - \zeta) = a - b\,\tan(\zeta). \tag{7}$$

A numerical procedure is given in Ref. [4] for calculating θ and R_c from the measured values of b, ζ, and a. For all of the experiments, the value of b was 3.05 mm and ζ was 50°. For each of our experiments, the measured value of a is given in Table I. The values of R_c and θ were constant in each experiment. Thus an iterative procedure could be used to determine their values. The value of R_c was assumed first and Eq. (2) integrated over ϕ until z_i reached the value $a - b\,\tan(\zeta)$. Since the argument of z_i at this point was equal to $\theta - \zeta$, the value of θ could be determined. Then Eq. (1) could be integrated until r_i had reached the value b, at which point its argument had the value $\theta - \zeta$. Thus a second value

TABLE I. Summary of the evaporation experiments with hydrocarbons.

Total liquid evaporation rate (μl/h)	Pressure in the vapor (Pa)	Temperature T_{M5} measured in the vapor near the interface at $(\hat{z}, 0)$[a] ($\pm$deviation)[b] (°C)	Temperature T_{NI}^{L} measured in the liquid near the interface at $(R_2^L, 0)$[a] ($\pm$deviation) (°C)	Average evaporation flux $\overline{j}$ (g m^{-2} s^{-1})	Height of the interface at the center a (mm)	Radius of the interface at the center R_c (mm)
440[c]	686.6	(6.03, 0)	(5.93, 0)	1.064	5.97	5.69
		11.9$\pm$0.0	8.8$\pm$0.2			
475[d]	2950.4	(5.96, 0)	(5.81, 0)	1.279	5.91	5.20
		13.4$\pm$0.2	10.9$\pm$0.2			
490[d]	2037.2	(5.71, 0)	(5.51, 0)	1.505	5.68	5.19
		7.2$\pm$0.2	4.2$\pm$0.2			
510[c]	530.6	(5.88, 0)	(5.73, 0)	1.305	5.87	5.09
		8.4$\pm$0.1	5.0$\pm$0.1			
550[c]	481.3	(5.85, 0)	(570, 0)	1.436	5.84	5.13
		6.8$\pm$0.0	3.2$\pm$0.0			
585[d]	1146.6	(5.31, 0)	(5.16, 0)	2.328	5.2	5.12
		$-$1.4$\pm$0.1	$-$5.8$\pm$0.1			
600[d]	1319.9	(5.21, 0)	(5.06, 0)	2.402	5.12	5.72
		0.7$\pm$0.1	$-$3.4$\pm$0.1			
630[c]	350.6	(5.66, 0)	(5.56, 0)	1.823	5.64	5.39
		3.8$\pm$0.2	0.1$\pm$0.1			
675[c]	318.6	(5.68, 0)	(5.53, 0)	1.929	5.66	5.67
		2.9$\pm$0.1	$-$1.7$\pm$0.1			
735[d]	686.6	(4.86, 0)	(4.71, 0)	2.912	4.83	4.50
		$-$7.3$\pm$0.1	$-$12.3$\pm$0.1			

[a]The unit of position used in the parentheses is mm.
[b]''$\pm$ deviation'' is the difference in the value of the temperatures from the mean mean measured one apart.
[c]Experiment with octane when the temperature of liquid entering the evaporation chamber was 26 °C.
[d]Methylcyclohexane experiment when the temperature of liquid entering the evaporation chamber was 26 °C.

of θ could be determined. If the two values of θ did not agree, then a new value of R_c was assumed and the process repeated. To assess the accuracy of the predicted area of the interface, the calculated interface shape $[z_i(\phi), r_i(\phi)]$ may be compared with the image captured by a charge coupled device camera. After the interface shape has been obtained, the surface area may be calculated from

$$A_I = \int_0^{\theta-\zeta} \frac{2\pi r_i}{\frac{2}{R_c} + \left(\frac{\rho^L g}{\gamma^{LV}}\right)\left((a - z_i) - \frac{\sin\phi}{r_i}\right)} d\phi. \quad (8)$$

For each experiment the calculated value of R_c is listed in Table I and the value of A_I in Table II. Then the average heat flux from the vapor phase to the interface may be expressed

$$\overline{Q}_{IV} = \frac{2\pi}{A_I} \int_0^{\theta-\zeta} \frac{r_i[-\kappa^V(\vec{\nabla}T)_{IV}\cdot\vec{n}_I]}{\left[\frac{2}{R_c} + \left(\frac{\rho^L g}{\gamma^{LV}}\right)\left(a - z_i - \frac{\sin\phi}{r_i}\right)\right]} d\phi, \quad (9)$$

where $\vec{n}_I$ is the unit normal vector of the interface. The value of $\overline{Q}_{IV}$ is used to determine one of the boundary conditions for the temperature field in the liquid.

IV. TEMPERATURE PROFILES

For these two hydrocarbons, the material properties are found in Ref. [6], which include the latent heat of vaporization, the densities of the saturation liquid and vapor, the saturation pressure, the viscosities of the liquid and the vapor, the surface tension, the thermal conductivities of the liquid and the vapor, and the specific heat at constant pressure. However, the molecular properties of these hydrocarbons, such as their quantum mechanical vibrational and rotational characteristics, are not available.

A. Temperature field in the vapor

Since the maximum Mach number in the highest evaporation experiments was 2.3×10^{-4}, the assumptions and the procedures for calculating the temperature profile in the vapor phase are the same as those described in Refs. [3] and [4]. The procedure is briefly described here. If the temperature nearest the interface in the liquid phase is denoted as T_{NI}^{L}, we take as the definition of nondimensional temperature $\overline{T}$,

$$\overline{T} = \frac{T(z,r) - T(z_2,0)}{T_{NI}^{L}}. \quad (10)$$

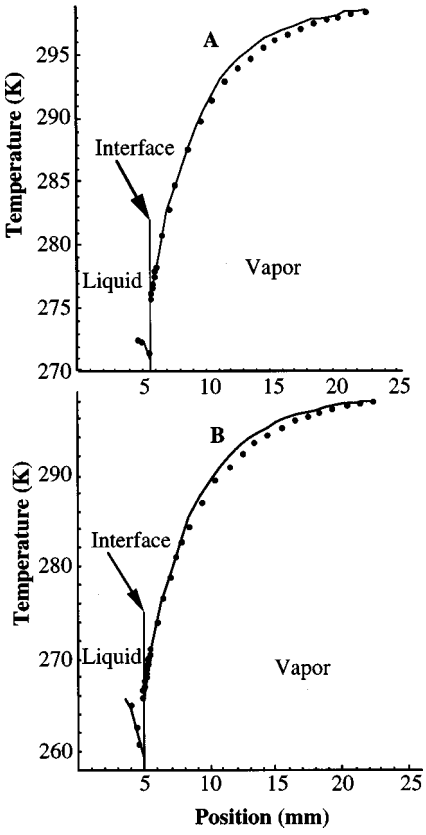

FIG. 2. Temperature profiles on the center line. The solid curve is the calculated temperature profile and the solid dots are the measured temperatures. The solid vertical line indicates the position of the interface. (a) Experiment with octane at a 675–μl/h liquid evaporation rate. (b) Experiment with methylcyclohexane at a 735-μl/h liquid evaporation rate.

Then the axisymmetric, steady-state continuum energy equation in cylindrical coordinates (z,r) may be written in terms of the nondimensional temperature

$$\mathrm{Pe}\,\frac{\partial}{\partial \bar{z}}\bar{T}=\frac{1}{\bar{r}}\frac{\partial}{\partial \bar{r}}\left(\bar{r}\frac{\partial}{\partial \bar{r}}\bar{T}\right)+\frac{\partial^2}{\partial \bar{z}^2}\,\bar{T}, \tag{11}$$

where the position coordinates have been nondimensionalized with respect to the radius of the evaporation chamber R_0 and the Péclet number Pe is given by

$$\mathrm{Pe}=\frac{\rho^V u R_0 c_p^V}{\kappa^V}, \tag{12}$$

where ρ^V is the density of the vapor, u is the fluid speed which we approximate as uniform, and c_p^V and κ^V are the constant pressure specific heat and the thermal conductivity of the vapor. The product $\rho^V u$ is the mass flux and it may be written in terms of the average evaporation flux $\bar{j}$. Since the area of the liquid-vapor interface A_I is different from the cross-sectional area of the evaporation chamber (see Fig. 1), the mass flux is given by

$$\rho^V u=\frac{\bar{j}A_I}{\pi R_0^2} \tag{13}$$

and P_e may then be expressed

$$P_e=\frac{\bar{j}A_I c_p^V}{\pi R_0 \kappa^V}. \tag{14}$$

For each experiment, the value of P_e may be calculated from Eq. (14) using the values [6] of c_p^V, κ^V, the results listed in Table II, and the value of R_0, which is equal to 9.5 mm [3].

If the temperatures measured at the positions $(z_2,0)$, (z_2,r_{w2}), and (z_1,r_{w1}) indicated in Fig. 1 are denoted as T_{M1}, T_{M2}, and T_{M3} and $\bar{T}_0$ is a value of the nondimensional temperature that is assigned to the position $(z_1,0)$, then following the procedure of Ref. [3], we assume that the temperature at the upper boundary of the vapor may be approximated as

$$\bar{T}(\bar{z}_2,\bar{r})=\bar{T}_{M1}+\bar{r}^2(\bar{T}_{M2}-\bar{T}_{M1}) \tag{15}$$

and at the bottom as

$$\bar{T}(\bar{z}_1,\bar{r})=\bar{T}_0+\bar{r}^2(\bar{T}_{M3}-\bar{T}_0). \tag{16}$$

As the boundary condition on the lateral surface of the vapor, we assume

$$\left(\frac{\partial \bar{T}}{\partial \bar{r}}\right)_{\bar{r}=1}=\frac{\mathrm{Nu}}{2}\,\bar{T}(\bar{z},1), \tag{17}$$

where Nu is the Nusselt number and may be expressed in terms of the heat transfer coefficient h: $\mathrm{Nu}=2R_0h/\kappa^V$. Following Refs. [3,4], the values of Nu and $\bar{T}_0$ are assigned by the procedure described below. For each experiment, we take Nu to be constant, but the value unknown for present. Then the solution to the energy equation may be written in terms of Bessel functions and after requiring the solution to be bounded on the axis, one finds

$$\bar{T}=\sum_{\lambda=0}^{\infty}(N_\lambda e^{m_1\bar{z}}+M_\lambda e^{m_2\bar{z}})J_0(q_\lambda \bar{r}), \tag{18}$$

where $J_0(q_\lambda \bar{r})$ is the zeroth-order Bessel function of the first kind. After applying the boundary condition given in Eqs. (15)–(17), one finds that the separation constant is given by

$$q_\lambda=-\frac{\mathrm{Nu}J_0(q_\lambda)}{2J_1(q_\lambda)} \tag{19}$$

and

$$m_1=\frac{\mathrm{Pe}-\sqrt{\mathrm{Pe}^2+4q_\lambda^2}}{2},\quad m_2=\frac{\mathrm{Pe}+\sqrt{\mathrm{Pe}^2+4q_\lambda^2}}{2} \tag{20}$$

and after taking advantage of the orthogonality properties of the Bessel functions

TABLE II. Values of Nu_B and $\overline{T}_{0B}$, maximum error of the calculation, and the temperature discontinuity across the interface.

Total liquid evaporation rate (μl/h)	Values of Nu_B and $\overline{T}_{0B}$	Temperature on the vapor side of the interface on the center line[a] ($\pm$deviation) (°C)	Temperature on the liquid side of the interface on the center line[a] ($\pm$deviation) (°C)	Interface area A_I (10^{-5} m^2)	Maximum difference of measured and calculated temperature on the center line (°C)	Maximum difference of measured and calculated temperature on the chamber wall (°C)	Temp difference across interface obtained with 25-μm TCs (°C)	Temp difference across interface obtained with 81-μm TCs (°C)
440[b]	17.04, −0.087	11.7 ±0.1	8.6 ±0.1	8.17	0.6	0.4	3.1±0.2	3.3±0.2
475[c]	18.44, −0.073	13.2 ±0.2	10.7 ±0.3	8.023	0.8	0.3	2.5±0.5	2.5±0.2
490[c]	17.07, −0.113	7.0 ±0.2	3.7 ±0.1	7.091	1.0	0.4	3.3±0.3	3.2±0.2
510[b]	16.74, −0.103	8.3 ±0.1	4.6 ±0.1	7.76	0.6	0.6	3.7±0.2	3.8±0.1
550[b]	17.07, −0.114	6.8 ±0.1	2.9 ±0.1	7.62	0.6	0.4	3.9±0.2	4.1±0.3
585[c]	16.83, −0.142	−2.1 ±0.0	−5.9 ±0.1	5.529	1.0	0.6	3.9±0.1	4.1±0.3
600[c]	17.00, −0.137	0.1 ±0.1	−3.5 ±0.1	5.479	0.9	0.5	3.6±0.2	3.8±0.3
630[b]	17.35, −0.127	3.7 ±0.2	−1.1 ±0.2	6.91	0.8	0.5	4.7±0.4	5.0±0.2
675[b]	16.95, −0.134	2.8 ±0.1	−2.1 ±0.1	7.00	0.6	0.6	4.9±0.2	5.1±0.3
735[c]	17.07, −0.165	−7.5 ±0.1	−13.3 ±0.3	4.452	1.0	0.6	5.7±0.4	5.9±0.2

[a]Temperature calculated at the interface.

[b]Experiment with octane when the temperature of liquid entering the evaporation chamber was 26 °C.

[c]Methylcyclohexane experiment when the temperature of liquid entering the evaporation chamber was 26 °C.

$$N_\lambda = 2\,\frac{e^{-m_2\overline{z}_1}\int_0^1 \overline{r}\,\overline{T}(\overline{z}_1,\overline{r})J_0(q_\lambda\overline{r})d\overline{r} - e^{-m_2\overline{z}_2}\int_0^1 \overline{r}\,\overline{T}(\overline{z}_2,\overline{r})J_0(q_\lambda\overline{r})d\overline{r}}{[J_1^2(q_\lambda)+J_0^2(q_\lambda)](e^{(m_1-m_2)\overline{z}_1}-e^{(m_1-m_2)\overline{z}_2})} \tag{21}$$

and

$$M_\lambda = \frac{2e^{-m_2\overline{z}_2}\int_0^1 \overline{r}\,\overline{T}(\overline{z}_2,\overline{r})J_0(q_\lambda\overline{r})d\overline{r}}{J_1^2(q_\lambda)+J_0^2(q_\lambda)} - N_\lambda e^{(m_1-m_2)\overline{z}_2}. \tag{22}$$

The values of N_λ and M_λ depend implicitly on the values of Nu and $\overline{T}_0$ and explicitly on P_e. To determine the values of N_λ and M_λ, we will use the measured evaporation flux and the temperatures measured in the vapor at five positions: $\overline{T}_{M1}$, $\overline{T}_{M2},\ldots,\overline{T}_{M5}$ listed in Table III. As indicated in Fig. 1, $\overline{T}_{M4}$ is the temperature measured at (z_3,r_{w3}) and $\overline{T}_{M5}$ is the temperature measured with the movable thermocouple at the position $(\hat{z},0)$. If the nondimensional temperature calculated at each of these positions is denoted as $\overline{T}_{Cj}$, $j=1,\ldots,5$, then a measure of the error between the calculated temperature and the measured temperature at these points is

$$E=\sum_{j=1}^{5}(\overline{T}_{Cj}-\overline{T}_{Mj})^2. \tag{23}$$

Since the calculated temperature depends on $\overline{T}_0$ and Nu as parameters, the best values to choose for these parameters would be those values that give the minimum error. This requires

$$\left(\frac{\partial E}{\partial\,\mathrm{Nu}}\right)_{\overline{T}_0=\overline{T}_{0B},\,\mathrm{Nu}=\mathrm{Nu}_B}=0 \tag{24}$$

and

TABLE III. Temperatures measured and $\overline{Q}_{IL}$ used in the boundary conditions.

Liquid evaporation rate (μl/h)	Position[a] (z,0) and temperature T_{M1} (°C)	Position[a] (z,r) and temperature T_{M2} (°C)	Position[a] (z,r) and temperature T_{M3} (°C)	Position[a] (z,r) and temperature T_{M4} (°C)	$\overline{Q}_{IL}$ (W/m^2)	Position[a] (R_1^L,0) and temperature T_1^L (°C)
440[b]	(22.53, 0)	(22.41, 8.13)	(15.88, 8.13)	(3.48, 8.13)	333.4	(4.03, 0)
	25.7±0.1	26.4±0.1	25.5±0.1	25.0±0.1	±0.2	9.6±0.1
475[c]	(22.46, 0)	(22.41, 8.13)	(15.88, 8.13)	(3.48, 8.13)	421.5	(4.46, 0)
	25.1±0.1	25.5±0.1	24.8±0.1	24.1±0.1	±1.1	11.4±0.3
490[c]	(22.51, 0)	(22.41, 8.13)	(15.88, 8.13)	(3.48, 8.13)	481.9	(4.01, 0)
	26.0±0.1	26.6±0.0	25.8±0.1	25.0±0.0	±1.4	6.1±0.1
510[b]	(22.53, 0)	(22.41, 8.13)	(15.88, 8.13)	(3.48, 8.13)	414.2	(4.03, 0)
	25.1±0.1	25.9±0.1	25.0±0.1	24.4±0.1	±0.2	5.9±0.0
550[b]	(22.50, 0)	(22.41, 8.13)	(15.88, 8.13)	(3.48, 8.13)	457.0	(4.50, 0)
	25.3±0.0	26.2±0.1	25.2±0.1	24.5±0.1	±0.0	4.8±0.0
585[c]	(22.56, 0)	(22.41, 8.13)	(15.88, 8.13)	(3.48, 8.13)	768.2	(4.06, 0)
	24.0±0.0	24.9±0.0	23.8±0.0	23.1±0.1	±1.1	−3.2±0.1
600[c]	(22.56, 0)	(22.41, 8.13)	(15.88, 8.13)	(3.48, 8.13)	797.3	(4.06, 0)
	26.2±0.1	27.0±0.0	25.9±0.0	25.0±0.1	±1.5	0.1±0.1
630[b]	(22.56, 0)	(22.41, 8.13)	(15.88, 8.13)	(3.48, 8.13)	593.6	(3.56, 0)
	25.4±0.0	26.3±0.0	25.2±0.1	24.4±0.1	±0.3	1.1±0.1
675[b]	(22.53, 0)	(22.41, 8.13)	(15.88, 8.13)	(3.48, 8.13)	632.4	(4.03, 0)
	25.4±0.1	26.5±0.1	25.3±0.1	24.4±0.0	±0.6	−0.5±0.0
735[c]	(22.46, 0)	(22.41, 8.13)	(15.88, 8.13)	(3.48, 8.13)	970.7±	(3.46, 0)
	25.0±0.1	26.0±0.0	24.7±0.1	23.8±0.1	1.2	−7.7±0.1

[a]The unit of position used in the parentheses is mm.
[b]Experiment with octane when the temperature of liquid entering the evaporation chamber was 26 °C.
[c]Methylcyclohexane experiment when the temperature of liquid entering the evaporation chamber was 26 °C.

$$\left(\frac{\partial E}{\partial \overline{T}_0}\right)_{\overline{T}_0=\overline{T}_{0B},\,\mathrm{Nu}=\mathrm{Nu}_B}=0. \tag{25}$$

Using the numerical procedure described in Ref. [4], the value of the P_e from Eq. (14) and the measured values of the temperatures at the five positions to obtain $\overline{T}_{Mj}$, $j=1,\ldots,5$ listed in Table III, the values of $\overline{T}_0$ and Nu may be determined from Eqs. (24) and (25). The values of $\overline{T}_0$ and Nu obtained for each experiment are listed in Table II. Once the values of $\overline{T}_0$ and Nu have been determined, they may be used to calculate the heat flux from the vapor to the liquid-vapor interface $\overline{Q}_V$.

B. Expressions for the temperature in the liquid

Spherical coordinates (R^L,φ,ω) are used to calculate the temperature field in the liquid. The axisymmetric energy equation in nondimensional form is

$$\overline{R}^2\frac{\partial^2\overline{T}}{\partial\overline{R}^2}+(2\overline{R}-\alpha)\frac{\partial}{\partial\overline{R}}\overline{T}+\frac{1}{\sin\varphi}\frac{\partial}{\partial\varphi}\left(\sin\varphi\frac{\partial}{\partial\varphi}\overline{T}\right)$$
$$=-\beta'\overline{R}^{-5}-\vartheta\cos\varphi, \tag{26}$$

where $\overline{T}$ is the ratio of the temperature in the liquid T^L to the temperature measured near the interface T_{NI}^L, the nondimensional radius $\overline{R}$ is the ratio of R^L to a,

$$\alpha\equiv\frac{\rho c_p j A_I}{2a\pi\kappa^L(1-\cos\varphi_{\max})}, \tag{27}$$

$$\beta'\equiv\frac{\rho(\overline{j}A_I)^3}{4a^5\pi^3\kappa^L(1-\cos\varphi_{\max})^3T_{NI}^L}, \tag{28}$$

and

$$\vartheta\equiv\frac{\rho g j\overline{A}_I}{2\pi\kappa^L(1-\cos\varphi_{\max})T_{NI}^L}, \tag{29}$$

where $\overline{j}$ is the measured evaporation flux, κ^L is the thermal conductivity of the liquid, and $\varphi_{\max}$ is the polar angle of the glass funnel. For the hydrocarbon experiments we consider, $\beta'\leqslant10^{-17}$ and $\vartheta\leqslant10^{-9}$; thus $\beta'\overline{R}^{-5}$ and $\vartheta\cos\varphi$ are negligible; however, the value of α is on the order of 0.20 and must be retained:

$$\frac{\partial^2\overline{T}}{\partial\overline{R}^2}+\frac{(2\overline{R}-\alpha)}{\overline{R}^2}\frac{\partial}{\partial\overline{R}}\overline{T}+\frac{1}{\overline{R}^2}\left(\frac{\partial^2\overline{T}}{\partial\varphi^2}+\cot\varphi\frac{\partial}{\partial\varphi}\overline{T}\right)=0. \tag{30}$$

Conservation of energy may be applied at the liquid-vapor interface to determine the boundary conditions. Since only the average evaporation flux has been measured, we take an average of the energy flux over the interface. The average energy flux from the vapor side to the interface $\overline{Q}_{IV}$ is deter-

mined from Eq. (9). As in the case of water, the value of the average energy flux at the interface in the liquid phase $\overline{Q}_{IL}$ may be determined from the measured evaporation flux $\overline{j}$

$$\overline{Q}_{IL}=\overline{j}(h^V-h^L)-\overline{Q}_{IV}, \tag{31}$$

where h is the enthalpy. We shall approximate the difference between h^V and h^L as the latent heat of vaporization λ_{LV}.

Because the liquid phase is inside the glass funnel and the funnel is inside the double-walled evaporation chamber, we again neglect the heat flux through the wall of the funnel. Thus the total heat flux averaged over a radial cross section in the liquid phase will be approximately constant throughout the liquid phase in a steady state.

To solve Eq. (30), a finite difference procedure [7] will be applied. In the finite difference procedure, the radial variable $\overline{R}$ and the azimuthal angle φ in spherical coordinates at a nodal point (i,j) are given by

$$\overline{R}=i\Delta\overline{R}, \quad i=\iota,\ldots,m \tag{32}$$

and

$$\varphi=j\Delta\varphi, \quad j=0,1,\ldots,n, \tag{33}$$

where $\iota\Delta\overline{R}$ is the distance corresponding to the position of R_1^L. The position R_1^L is the position on the center line deepest in the liquid where the temperature was measured. The temperature at a point (i,j) may be expressed

$$\overline{T}(\overline{R},\varphi)|_{i,j}=\overline{T}(i\Delta\overline{R},j\Delta\varphi)=\overline{T}_{i,j}. \tag{34}$$

The temperatures at the neighboring nodal points surrounding the point (i,j) (five-point formula) are expressed by applying a Taylor series at (i,j) and neglecting the terms containing third- or higher-order derivatives:

$$\overline{T}_{i+1,j}=\overline{T}_{i,j}+(\Delta\overline{R})\left(\frac{\partial}{\partial\overline{R}}\overline{T}\right)_{i,j}+\frac{(\Delta\overline{R})^2}{2}\left(\frac{\partial^2\overline{T}}{\partial\overline{R}^2}\right)_{i,j}, \tag{35}$$

$$\overline{T}_{i-1,j}=\overline{T}_{i,j}-(\Delta\overline{R})\left(\frac{\partial}{\partial\overline{R}}\overline{T}\right)_{i,j}+\frac{(\Delta\overline{R})^2}{2}\left(\frac{\partial^2\overline{T}}{\partial\overline{R}^2}\right)_{i,j}, \tag{36}$$

$$\overline{T}_{i,j+1}=\overline{T}_{i,j}+(\overline{R}\Delta\varphi)\left(\frac{\partial}{\partial(\overline{R}\varphi)}\overline{T}\right)_{i,j}+\frac{(\overline{R}\Delta\varphi)^2}{2}\left(\frac{\partial^2\overline{T}}{\partial(\overline{R}\varphi)^2}\right)_{i,j}, \tag{37}$$

and

$$\overline{T}_{i,j-1}=\overline{T}_{i,j}-(\overline{R}\Delta\varphi)\left(\frac{\partial}{\partial(\overline{R}\varphi)}\overline{T}\right)_{i,j}+\frac{(\overline{R}\Delta\varphi)^2}{2}\left(\frac{\partial^2\overline{T}}{\partial(\overline{R}\varphi)^2}\right)_{i,j}. \tag{38}$$

We multiply both sides of Eqs. (35)–(38) by A, B, C, and D, respectively, add the resulting expressions, and collect the terms involving derivatives on one side:

$$\begin{aligned}&A(\overline{T}_{i+1,j}-\overline{T}_{i,j})+B(\overline{T}_{i-1,j}-\overline{T}_{i,j})\\&\quad+C(\overline{T}_{i,j+1}-\overline{T}_{i,j})+D(\overline{T}_{i,j+1}-\overline{T}_{i,j})\\&=(A-B)(\Delta\overline{R})\left(\frac{\partial}{\partial\overline{R}}\overline{T}\right)_{i,j}\\&\quad+(A+B)\frac{(\Delta\overline{R})^2}{2}\left(\frac{\partial^2\overline{T}}{\partial\overline{R}^2}\right)_{i,j}\\&\quad+(C-D)(\overline{R}\Delta\varphi)\left(\frac{\partial}{\partial(\overline{R}\varphi)}\overline{T}\right)_{i,j}\\&\quad+(C+D)\frac{(\overline{R}\Delta\varphi)^2}{2}\left(\frac{\partial^2\overline{T}}{\partial(\overline{R}\varphi)^2}\right)_{i,j}.\end{aligned} \tag{39}$$

The side with the derivative terms represents Eq. (30). By comparing the coefficients of Eq. (39) with those of Eq. (30), the four coefficients A, B, C, and D may be determined:

$$A=\frac{1}{(\Delta\overline{R})^2}+\frac{2i\Delta\overline{R}-\alpha}{2i^2(\Delta\overline{R})^3}, \tag{40}$$

$$B=\frac{1}{(\Delta\overline{R})^2}-\frac{2i\Delta\overline{R}-\alpha}{2i^2(\Delta\overline{R})^3}, \tag{41}$$

$$C=\frac{1}{(i\Delta\overline{R}\Delta\varphi)^2}+\frac{\cot(j\Delta\varphi)}{2(i\Delta\overline{R})^2\Delta\varphi}, \tag{42}$$

and

$$D=\frac{1}{(i\Delta\overline{R}\Delta\varphi)^2}-\frac{\cot(j\Delta\varphi)}{2(i\Delta\overline{R})^2\Delta\varphi}. \tag{43}$$

Then A, B, C, and D are substituted into Eq. (39) and one finds for $\iota+1\leq i\leq m-1$ and $1\leq j\leq n-1$

$$\left(1+\frac{2i\Delta\overline{R}-\alpha}{2i^2(\Delta\overline{R})}\right)\overline{T}_{i+1,j}+\left(1-\frac{2i\Delta\overline{R}-\alpha}{2i^2(\Delta\overline{R})}\right)\overline{T}_{i-1,j}$$
$$-2\overline{T}_{i,j}-\frac{2\overline{T}_{i,j}}{(i\Delta\varphi)^2}+\left(\frac{1}{(i\Delta\varphi)^2}+\frac{\cot(j\Delta\varphi)}{2i^2\Delta\varphi}\right)\overline{T}_{i,j+1}$$
$$+\left(\frac{1}{(i\Delta\varphi)^2}-\frac{\cot(j\Delta\varphi)}{2i^2\Delta\varphi}\right)\overline{T}_{i,j-1}=0. \quad (44)$$

To examine the error of the finite difference procedure, we will compare the calculated temperature profile with the temperature measured on the center line.

On the central line ($\varphi=0$ and $j=0$), one has

$$\lim_{\varphi\to 0}\left(\cot\varphi\,\frac{\partial}{\partial\varphi}\overline{T}\right)=\frac{\partial^2\overline{T}}{\partial\varphi^2}. \quad (45)$$

Substituting Eq. (45) into Eq. (30), one finds

$$\frac{\partial^2\overline{T}}{\partial\overline{R}^2}+\frac{(2\overline{R}-\alpha)}{\overline{R}^2}\frac{\partial}{\partial\overline{R}}\overline{T}+\frac{2}{\overline{R}^2}\left(\frac{\partial^2\overline{T}}{\partial\varphi^2}\right)=0. \quad (46)$$

Since the temperature profile was assumed to be axially symmetric,

$$\overline{T}_{i,-1}=\overline{T}_{i,1}. \quad (47)$$

Following the same procedure, Eq. (46) may be written for $j=0$ and $\iota+1\leqslant i\leqslant m-1$,

$$\left(1+\frac{2i\Delta\overline{R}-\alpha}{2i^2(\Delta\overline{R})}\right)\overline{T}_{i+1,0}+\left(1-\frac{2i\Delta\overline{R}-\alpha}{2i^2(\Delta\overline{R})}\right)\overline{T}_{i-1,0}$$
$$-2\overline{T}_{i,0}+\frac{4(\overline{T}_{i,1}-\overline{T}_{i,0})}{(i\Delta\varphi)^2}=0. \quad (48)$$

On the wall of the glass funnel ($\varphi=\varphi_{\max}$ and $j=n$), the energy transfer through the wall is negligible and one has

$$\left(\frac{\partial}{\partial(\overline{R}\varphi)}\overline{T}\right)_{i,n}=0. \quad (49)$$

If Eq. (49) is used to replace Eq. (37), then for $j=n$ and $\iota+1\leqslant i\leqslant m-1$, the energy equation becomes

$$\left(1+\frac{2i\Delta\overline{R}-\alpha}{2i^2(\Delta\overline{R})}\right)\overline{T}_{i+1,n}+\left(1-\frac{2i\Delta\overline{R}-\alpha}{2i^2(\Delta\overline{R})}\right)\overline{T}_{i-1,n}$$
$$-2\overline{T}_{i,n}+\frac{2(\overline{T}_{i,n-1}-\overline{T}_{i,n})}{(i\Delta\varphi)^2}=0. \quad (50)$$

At the surface defined by

$$\overline{R}=R_1^L/a, \quad (51)$$

i has its minimum value ι. On this surface the temperature gradient may be obtained from the assumption that the total heat flux through the liquid bulk phase is constant [3]:

$$\left(\frac{\partial}{\partial\overline{R}}\overline{T}\right)_{\iota,j}=-\frac{\overline{Q}_{IL}A_I}{2\pi a\kappa^L(\iota\Delta\overline{R})^2T_{NI}^L(1-\cos\varphi_{\max})} \quad (52)$$

and Eq. (36) must be replaced by Eq. (52). Then Eq. (52) may be solved with Eqs. (35), (37), and (38) for $1\leqslant j\leqslant n-1$ to obtain

$$2(\overline{T}_{\iota+1,j}-\overline{T}_{\iota,j})-\frac{\overline{Q}_{IL}A_I}{2\pi a\kappa^L\iota^2T_{NI}^L(1-\cos\varphi_{\max})}$$
$$\times\left(\frac{2\iota\Delta\overline{R}-\alpha}{(\iota\Delta\overline{R})^2}-\frac{2}{\Delta\overline{R}}\right)-\frac{2\overline{T}_{\iota,j}}{(\iota\Delta\varphi)^2}$$
$$+\left(\frac{1}{(\iota\Delta\varphi)^2}+\frac{\cot(j\Delta\varphi)}{2\iota^2\Delta\varphi}\right)\overline{T}_{\iota,j+1}$$
$$+\left(\frac{1}{(\iota\Delta\varphi)^2}-\frac{\cot(j\Delta\varphi)}{2\iota^2\Delta\varphi}\right)\overline{T}_{\iota,j-1}=0. \quad (53)$$

At the position on the funnel wall where

$$\overline{R}=(R_1^L/a),\quad \varphi=\varphi_{\max} \quad (54)$$

the indices have the values

$$i=\iota,\quad j=n$$

and the temperature gradient in the φ direction is zero,

$$\left(\frac{\partial}{\partial(\overline{R}\varphi)}\overline{T}\right)_{\iota,n}=0. \quad (55)$$

At this position, in the R direction

$$\left(\frac{\partial}{\partial\overline{R}}\overline{T}\right)_{\iota,n}=-\frac{\overline{Q}_{IL}A_I}{2\pi a\kappa^L(\iota\Delta\overline{R})^2T_{NI}^L(1-\cos\varphi_{\max})}. \quad (56)$$

If Eqs. (36) and (37) are replaced by Eqs. (56) and (55), then for $i=\iota$ and $j=n$ one finds

$$2(\overline{T}_{\iota+1,n}-\overline{T}_{\iota,n})-\frac{\overline{Q}_{IL}A_I}{2\pi a\kappa^L\iota^2T_{NI}^L(1-\cos\varphi_{\max})}$$
$$\times\left(\frac{2\iota\Delta\overline{R}-\alpha}{(\iota\Delta\overline{R})^2}-\frac{2}{\Delta\overline{R}}\right)+\frac{2(\overline{T}_{\iota,n-1}-\overline{T}_{\iota,n})}{(\iota\Delta\varphi)^2}=0. \quad (57)$$

To establish the boundary condition at the interface, it is assumed that the interface may be approximated as spherical ($i=m$) and that the temperature gradient obeys the same formula as that given in Eq. (52),

$$\left(\frac{\partial}{\partial \overline{R}}\overline{T}\right)_{m,j} = -\frac{a\overline{Q}_{IL}}{\kappa^L T^L_{NI}}. \tag{58}$$

If Eq. (35) is replaced by Eq. (58), then for $i=m$ and $1\leqslant j \leqslant n-1$ one finds

$$2(\overline{T}_{m-1,j}-\overline{T}_{m,j}) - \frac{a\overline{Q}_{IL}}{\kappa^L T^L_{NI}}\left(\frac{2m\Delta\overline{R}-\alpha}{m^2}+2\Delta\overline{R}\right) - \frac{2\overline{T}_{m,j}}{(m\Delta\varphi)^2} + \left(\frac{1}{(m\Delta\varphi)^2}+\frac{\cot(j\Delta\varphi)}{2m^2\Delta\varphi}\right)\overline{T}_{m,j+1} + \left(\frac{1}{(m\Delta\varphi)^2}-\frac{\cot(j\Delta\varphi)}{2m^2\Delta\varphi}\right)\overline{T}_{m,j-1}=0. \tag{59}$$

At the interface and on the funnel wall ($i=m$ and $j=n$), the temperature gradient in the φ direction through the wall is zero,

$$\left(\frac{\partial}{\partial(\overline{R}\varphi)}\overline{T}\right)_{m,n} = 0, \tag{60}$$

and

$$\left(\frac{\partial}{\partial \overline{R}}\overline{T}\right)_{m,n} = -\frac{a\overline{Q}_{IL}}{\kappa^L T^L_{NI}}. \tag{61}$$

For $i=m$ and $j=n$ one has

$$2(\overline{T}_{m-1,n}-\overline{T}_{m,n}) - \frac{a\overline{Q}_{IL}}{\kappa^L T^L_{NI}}\left(\frac{2m\Delta\overline{R}-\alpha}{m^2}+2\Delta\overline{R}\right) + \frac{2(\overline{T}_{m,n-1}-\overline{T}_{m,n})}{(m\Delta\varphi)^2}=0. \tag{62}$$

To calculate the temperature field in the liquid phase, the temperature expressions given in Eqs. (44), (48), (50), (53), (57), (59), and (62) may be used. For these $m-\iota+n+1$ equations, there are $m-\iota+n+3$ unknowns. The number of unknowns may be reduced to the number of equations by noting that the temperature $T(\iota,0)$ at the position $(R^L_1,0)$ is measured in the experimental procedure and by hypothesizing a value of the temperature at the interface in the liquid $T(m,0)$.

Once the values of these temperatures have been introduced, the calculation may be performed. The number of nodals for m and n is set to 12 and 4, respectively (the number of nodal for m may be adjusted ± 1 if the position of ι is not at the same position where a temperature was measured). The assumed value of $T(m,0)$ may then be examined by comparing the temperature calculated at the position $(R^L_2,0)$ with the measured value there. If the agreement is not satisfactory, the value of $T(m,0)$ may be adjusted and the calculation repeated. In the calculations reported below, the procedure was continued until the agreement was within 0.2 K.

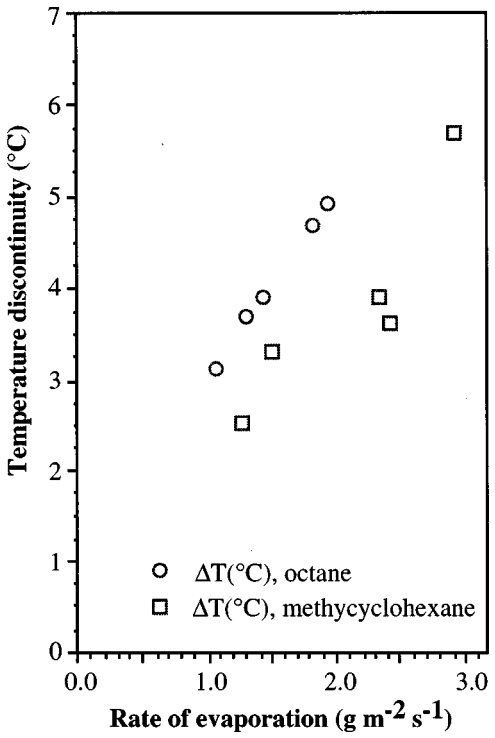

FIG. 3. Temperature discontinuity measured across the liquid-vapor interface for the experiments with two hydrocarbons when evaporation was occurring at the indicated rate.

V. TEMPERATURE DISCONTINUITY AT THE INTERFACE

The temperatures measured at the boundaries and used in the calculations of the temperature are listed in Table III. At the highest evaporation rate for each liquid, the calculated temperature profiles on the center line are shown in Fig. 2. The maximum difference between the calculated and measured temperature at any position is 1.0 °C.

The temperatures calculated at the interface are listed in Table II and the temperature discontinuities at the interface for all experiments are shown in Fig. 3. Note that in each case the temperature was greater in the vapor than in the liquid. Also, the magnitude of the temperature discontinuity at the interface for methylcyclohexane evaporation is slightly smaller than that for octane evaporation at the same rate of evaporation.

To examine the effect of the temperature gradient on the thermocouple reading, a second thermocouple of the same type but of different size (81.3-μm-diam wire) was used to measure the temperature on the center line. The temperature discontinuity based on the measurement with the large thermocouple is also listed in Table II. The temperature measurements with the large thermocouple were used in the analytical procedure described in Sec. IV to calculate the temperature in the liquid and in the vapor at the interface. The maximum difference in the temperature discontinuity with the differently sized thermocouples is 0.3 °C.

Of the 30 measurements of temperature on the center line, only two were used in the calculation of the temperature field in each phase. Thus the accuracy of the calculated temperature field can be evaluated by comparing the measurements made at other positions on the center line with those calcu-

lated there. The maximum error at any position is within 1 °C (see Table II).

VI. PREDICTED EXPRESSION FOR THE EVAPORATION FLUX

To predict the evaporation flux, the SRT procedure considers the transfer of molecules across an element of interfacial area δA from a small volume of liquid, extent δL^L and temperature T^L, to a small volume of vapor, extent δL^V and temperature T^V. Each volume is assumed to be described in terms of the local equilibrium variables and at one instant to consist of known numbers of molecules $\delta N^L, \delta N^V$. Thus, at one instant each small volume may be treated as a canonical ensemble system. Then the uncertainty in the energy of each volume ΔE^α would be given by

$$\Delta E^\alpha = \pm T^\alpha \sqrt{k C_V^\alpha}, \quad \alpha = L, V, \tag{63}$$

where k is the Boltzmann constant and C_V^α is the constant volume specific heat of phase α. The total uncertainty in the energy ΔE is the sum of ΔE^L and ΔE^V.

The probability of a change in the molecular configuration at any instant in the period δt from a particular molecular distribution to a molecular distribution in which one molecule has been transferred to the vapor volume can be obtained from the first-order perturbation analysis. The expression for this transition probability can be used to obtain the expression for the evaporation flux j [2] provided

$$\frac{\delta L^\alpha}{v^\alpha j} \gg \delta t \gg \frac{2\pi\hbar}{\Delta E^L + \Delta E^V}, \tag{64}$$

where $\hbar$ is the Planck constant divided by 2π and the specific volume v^α of phase α. One finds

$$j = \frac{\eta P_\infty(T^L)}{\sqrt{2\pi m k T^L}} \left(\exp \frac{\Delta S}{k} - \exp \frac{-\Delta S}{k} \right), \tag{65}$$

where $P_\infty(T^L)$ is the saturation pressure corresponding to the temperature T^L, m is the mass of the molecule, and since the vapor has been assumed to be an ideal gas η is given by

$$\eta = \exp\left(\frac{v_\infty^L}{k T^L} [P_e^L - P_\infty(T^L)] \right). \tag{66}$$

If the pressure of the liquid phase is not too different from the saturation vapor pressure, i.e., if

$$\kappa^L |P^L - P_\infty(T^L)| \ll 1, \tag{67}$$

where κ^L is the isothermal compressibility of the liquid, this phase may be approximated as slightly compressible. Then its chemical potential is given by

$$\mu(T,P) = \mu[T^L, P_\infty(T^L)] + v_\infty^L [P - P_\infty(T^L)]. \tag{68}$$

If R_1 and R_2 are the radii of curvature of the surface element δA, the value of P_e^L is determined by solving iteratively

$$P_e^L - \gamma^{LV}\left(\frac{1}{R_1} + \frac{1}{R_2} \right) = P_\infty(T^L) \exp\left[\frac{v_\infty^L}{k T^L} [P_e^L - P_\infty(T^L)] \right]. \tag{69}$$

The change in entropy that results from one molecule transferring from the liquid to the vapor ΔS is given by

$$\Delta S = \left(\frac{\mu^L}{T^L} - \frac{\mu^V}{T^V} \right) + h^V \left(\frac{1}{T^V} - \frac{1}{T^L} \right). \tag{70}$$

If Boltzmann statistics are used and the Born-Oppenheimer approximation introduced, then the expression for the enthalpy per molecule of the vapor is given by [8]

$$h^V = 4kT^V - D_e + k \sum_{l=1}^{n'} \frac{\Theta_l}{2} + k \sum_{l=1}^{n'} \frac{\Theta_l}{\exp(\Theta_l / T^V) - 1}, \tag{71}$$

where n' is the number of vibrational degrees of freedom. Also, the expression for the chemical potential is given by

$$\frac{\mu^V(T,P)}{T} = -k \ln\left[\left(\frac{m}{2\pi\hbar^2} \right)^{3/2} \frac{(kT)^{5/2}}{P} \right] - k \ln(q_{\text{vib}} q_{\text{rot}} q_{\text{elec}}). \tag{72}$$

The electronic partition function is given by

$$q_{\text{elec}} = g_e \exp\left(\frac{D_e}{kT} \right), \tag{73}$$

where g_e and D_e are the degeneracy of the state and the reference potential minimum. The vibrational and the rotational partition functions for the ideal polyatomic molecules may be expressed

$$q_{\text{vib}} = \prod_{l=1}^{n'} \frac{\exp(-\Theta_l / 2T)}{1 - \exp(-\Theta_l / T)} \tag{74}$$

and

$$q_{\text{rot}} = \left(\frac{2kT}{\hbar^2} \right)^{1.5} \frac{(\pi I)^{0.5}}{\sigma_s}, \tag{75}$$

where Θ_l is a characteristic temperature for vibration, I is the product of principal moments of inertia of the molecule, and σ_s the symmetry factor of the vibration orientation. At the saturation condition, the chemical potential of the liquid and vapor phases are equal:

$$\mu^L[T^L, P_\infty(T^L)] = \mu^V[T^L, P_\infty(T^L)]. \tag{76}$$

Thus from Eq. (72)

$$\frac{\mu^V[T^L, P_\infty(T^L)]}{T^L} = -k \ln\left[\left(\frac{m}{2\pi\hbar^2} \right)^{3/2} \frac{(kT^L)^{5/2}}{P_\infty(T^L)} \right] - k \ln[q_{\text{vib}}(T^L) q_{\text{rot}}(T^L) q_{\text{elec}}(T^L)] \tag{77}$$

and from Eqs. (68), (72), and (77)

$$\frac{\mu^L(T^L,P^L)}{T^L}-\frac{\mu^V(T^V,P^V)}{T^V}$$
$$=\frac{v_\infty^L}{T^L}\left[P^V+\gamma^{LV}\left(\frac{1}{R_1}+\frac{1}{R_2}\right)-P_\infty(T^L)\right]$$
$$-D_e\left(\frac{1}{T^L}-\frac{1}{T^V}\right)+k\ \ln\left[\left(\frac{T^V}{T^L}\right)^{5/2}\left(\frac{P_\infty(T^L)}{P^V}\right)\right]$$
$$+k\ \ln\left(\frac{q_{\rm rot}(T^V)q_{\rm vib}(T^V)}{q_{\rm rot}(T^L)q_{\rm vib}(T^L)}\right). \tag{78}$$

After substituting Eqs. (71) and (78) into Eq. (70) one finds

$$\frac{\Delta S}{k}=4\left(1-\frac{T^V}{T^L}\right)+\left(\frac{1}{T^V}-\frac{1}{T^L}\right)$$
$$\times\sum_{l=1}^{3}\left(\frac{\Theta_l}{2}+\frac{\Theta_l}{\exp(\Theta_l/T^V)-1}\right)$$
$$+\ln\left[\left(\frac{T^V}{T^L}\right)^{5/2}\frac{P_\infty(T^L)}{P^V}\right]$$
$$+\frac{v_\infty^L}{kT^L}\left[P^V+\gamma^{LV}\left(\frac{1}{R_1}+\frac{1}{R_2}\right)-P_\infty(T^L)\right]$$
$$+\ln\left(\frac{q_{\rm rot}(T^V)q_{\rm vib}(T^V)}{q_{\rm rot}(T^L)q_{\rm vib}(T^L)}\right). \tag{79}$$

Since the vibrational and the rotational temperatures that appear in the partition functions are not available for the hydrocarbons, we shall investigate the possibility of neglecting changes in rotational and vibrational partition functions that result from changing the temperature from T^L to T^V. Under this condition, ΔS becomes

$$\frac{\Delta S}{k}=4\left(1-\frac{T^V}{T^L}\right)+\frac{v_\infty^L}{kT^L}\left[P^V+\gamma^{LV}\left(\frac{1}{R_1}+\frac{1}{R_2}\right)-P_\infty(T^L)\right]$$
$$+\ln\left[\left(\frac{T^V}{T^L}\right)^{5/2}\frac{P_\infty(T^L)}{P^V}\right]. \tag{80}$$

Once Eqs. (66) and (80) are substituted into Eq. (65), one obtains an expression for the evaporation flux that is in terms of T^L, T^V, P^V, R_1, and R_2.

VII. EXAMINATION OF THE EXPRESSION FOR THE EVAPORATION FLUX

The rate of evaporation was set by a computer controlled syringe pump (accuracy $\pm 0.5\%$), the temperatures at the interface are accurately predicted (see Fig. 2), and for the hydrocarbon interfaces that we consider, the evaporation flux is insensitive to the radii of curvature; however, the pressure in the vapor could only be measured to 13.3 Pa. A sensitivity analysis has been performed on the SRT expression for the evaporation rate. In order for the evaporation rate to be predicted as accurately as it could be measured for the experiment with the highest evaporation rate, for octane the pressure would have to be measured to within 0.0017 Pa and for methylcyclohexane to within 0.0026 Pa.

Thus, to examine the validity of the expression for the evaporation flux, we shall use the expression for the flux to predict the value of the pressure in the vapor at which evaporation would occur at a measured rate. Also, in making this prediction, we assume the liquid-vapor interface will be approximated as spherical:

$$R_1=R_2=R_c. \tag{81}$$

The value of R_c and the average value of j for each experiment are given in Table I and the values of T^V and T^L on the center line are given in Table II. When these values are substituted into Eq. (65), the value of the pressure for each experiment can be predicted. The results obtained for both hydrocarbons are shown in Fig. 4.

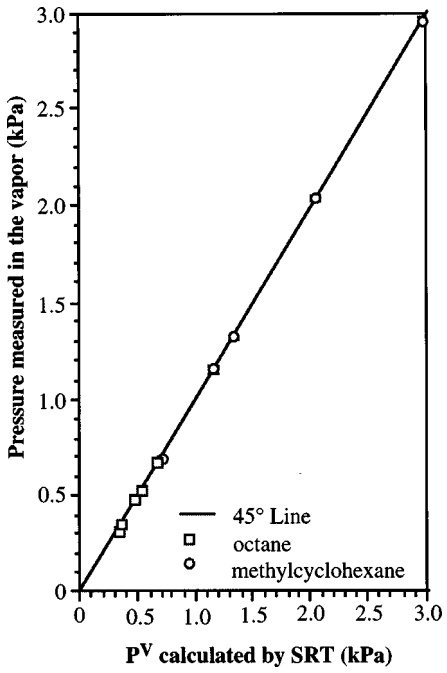

FIG. 4. Comparison of the pressure in the vapor predicted by the SRT approach and with that measured in the vapor phase. The open squares represent the experiments with octane and the open circles represent the experiments with methylcyclohexane. If there were perfect agreement between the measurements and the predictions, all points would lie on the solid 45° line. The error in the measured pressure was ± 13.3 Pa, but this is too small to be indicated.

The pressure in the vapor was not measured exactly at the interface; however, the maximum Mach number in these experiments was 2.0×10^{-4}. Thus the effect of the vapor bulk velocity on the pressure reading would be less than 1.0 Pa. The error for the measurement of the pressure in the vapor is 13.3 Pa. Thus the effect of the position at which the pressure was measured would be small compared to the accuracy of the measurement. Hence, to examine the validity of the SRT expression for the evaporation flux, the measured pressure in the vapor may be directly compared with the predicted pressure on the vapor side of the interface. The measured values of the pressures for each experiment are also shown in Fig. 4, where they may be directly compared with the predicted values.

Clearly, the measurements and the predictions are in very close agreement. Because of the large values of the pressure in these cases, the error bars on the measured pressure are not visible. In none of the experiments with either octane or methylcyclohexane did the predicted pressure differ from the

measured pressure by as much as 13.3 Pa. Thus there was no measured difference between the predictions and the measurements for either hydrocarbon.

VIII. DISCUSSION AND CONCLUSION

The SRT expression for the evaporation flux is based on the transition probability concept. This concept can be justified from a first-order perturbation analysis of the Schrödinger equation if the time δt for a molecule to make a transition from the liquid phase to the vapor satisfies Eq. (64) [2]. To examine the limits on δt, the extent of the small volume in the vapor δL^V will be approximated as the mean free path and its value may be estimated from the viscosity of the vapor. The value of ΔE^α may be calculated from Eq. (63). The most stringent condition arises when the evaporation flux is the highest. Using the values of the evaporation flux, the temperatures listed in Table I, and the values of the thermodynamic properties in Ref. [6], one finds for octane that

$$3\times 10^{-6} \gg \delta t(s^{-1}) \gg 3\times 10^{-14} \tag{82}$$

and for methylcyclohexane that

$$2\times 10^{-5} \gg \delta t(s^{-1}) \gg 3\times 10^{-14}. \tag{83}$$

Thus the necessary condition for calculating the transition probability from a first-order perturbation analysis of the Schrödinger equation appears to be satisfied.

The sufficient condition for the validity can only be established by comparing the predictions with the measurements. In each of the five experiments with two hydrocarbons, the temperature in the vapor at the interface has been found to be greater than that in the liquid at the interface. The maximum discontinuity in the case of octane was 4.7 °C and for methylcyclohexane it was 5.7 °C. When these temperatures are inserted into the SRT expression for the evaporation flux and the value of the pressure in the vapor calculated that would produce the observed evaporation rate, it was found in five experiments with octane and five with methylcyclohexane that there was no measured disagreement.

The measured temperature discontinuity for these hydrocarbons is in the same direction as that found for water. For all three liquids, there is close agreement between the predictions from the SRT expression for the liquid evaporation rate and the measurements [2]. In the case of water, the temperature discontinuity is in the opposite direction to that predicted by classical kinetic theory. One question that arises is whether quantum mechanics plays an essential role in the predictions that are in agreement with the measurements. How the SRT expression [i.e., Eqs. (65) and (70)] could be derived from a classical point of view is unclear. Also, we note that the energy uncertainty principle plays an essential role in its derivation. If one adopted a classical thermodynamic description of the small volume of liquid or of vapor, then since each small volume was assumed to have a known temperature T^α, a known volume $\delta L^\alpha \delta A$, and known number of particles N^α, the small volume would necessarily have a certain energy. Thus, in the classical limit both the Planck constant and ΔE^α would be zero. This would mean that the procedure for deriving the SRT expression for the evaporation rate from a first-order perturbation analysis of the Schrödinger equation could not be justified since the right-hand side of Eq. (65) would become undefined (i.e., 0/0).

If the SRT expression were available, it could not be correctly evaluated from a strictly classical point of view because the molecules would be viewed as distinguishable. This point of view has a profound effect on the expression for the chemical potential because this function then depends on the extensive variables rather than only intensive variables. For example, the chemical potential of a classical monatomic ideal gas of distinguishable particles is

$$\mu^{\mathrm{cl}} = -kT \ln[V(2\pi mkT)^{3/2}]. \tag{84}$$

In this circumstance, the procedure used in Eqs. (76) and (77) could not be used to express

$$\frac{\mu^L(T^L,P^L)}{T^L} - \frac{\mu^V(T^V,P^V)}{T^V} \tag{85}$$

in terms of the intensive properties at the interface. One would find that this difference in chemical potentials depended on the sizes chosen for the small volumes and such a result would be completely nonphysical. However, it has been known since the time of Gibbs that the expression for the chemical potential that is obtained from strictly classical mechanics has to be ''corrected'' [9]. The correction is derived from quantum mechanics without special consideration simply by taking the indistinguishability of the molecules into account. In general, one can say that strictly classical statistical mechanics does not provide the correct dependence on the number of particles in the expression for the thermodynamic properties. Thus, in this sense, it appears that quantum mechanics plays a fundamental role in determining the expression for the evaporation rate; however, it is not clear that this is the cause of the predictions of classical kinetic theory being in disagreement with the measurements.

ACKNOWLEDGMENTS

This work was completed with the support of the Natural Sciences and Engineering Research Council of Canada, and the Canadian Space Agency.

[1] C. A. Ward, J. Chem. Phys. **67**, 229 (1977); C. A. Ward, R. D. Findlay, and M. Rizk, *ibid.* **76**, 5599 (1982); C. A. Ward, *ibid.* **79**, 5605 (1983); C. A. Ward and M. Elmoselhi, Surf. Sci. **176**, 457 (1986); J. A. W. Elliott and C. A. Ward, J. Chem. Phys. **106**, 5667 (1997); **106**, 5667 (1997).

[2] C. A. Ward and G. Fang, preceding paper, Phys. Rev. E **58**, 429 (1999).

[3] G. Fang and C. A. Ward, this issue, Phys. Rev. E **58**, 417 (1999).

[4] C. A. Ward and G. Fang (unpublished).

[5] Y.-P. Pao, Phys. Fluids **14**, 306 (1971); **16**, 1560(E) (1971); **16**, 1340 (1973); C. E. Siewert and J. R. Thomas, Jr., *ibid.* **16**, 1557 (1973); K. Aoki and C. Cercignani, *ibid.* **26**, 1163 (1983); J. W. Cipolla, Jr., H. Lang, and S. K. Loyalka, J. Chem. Phys. **61**, 69 (1974).

[6] N. B. Vargaftik, *Tables on the Thermophysical Properties of Liquids and Gases in Normal and Dissociated States*, 2nd ed. (Hemisphere, New York, 1975), pp. 269 and 303; N. V. Tsederberg, *Thermal Conductivity of Gases and Liquids* (MIT Press, Cambridge, MA, 1965), pp. 89 and 137; C. Y. Ho, P. E. Liley, T. Makita, and Y. Tanaka, *Properties of Inorganic and Organic Fluids, CINDAS Data Series on Material Properties* (Hemisphere, New York, 1988), Vol. 1, p. 245; D. J. Jamieson, J. B. Irving, and J. S. Tudhope, *Liquid Thermal Conductivity, A Data Survey to 1973* (National Engineering Library, Her Majesty's Stationery Office, Edinburgh, 1975), pp. 41, 61, and 66; C. L. Yaws, *Handbook of Viscosity, Organic Compounds C_5 to C_7* (Gulf, Houston, 1995), Vol. 2, p. 329; Y. M. Naziev and A. N. Shakhverdiyev, in *Thermal Conductivity 17*, edited by J. G. Hust (Plenum, New York, 1981), p. 275.

[7] M. N. Ozisik, *Boundary Value Problems of Heat Conduction* (Dover, New York, 1989), p. 412; W. J. Minkowycz, E. M. Sparrow, G. E. Schneider, and R. H. Pletcher, *Handbook of Numerical Heat Transfer* (Wiley, New York, 1988), p. 53.

[8] T. L. Hill, *An Introduction to Statistical Thermodynamics* (Dover, New York, 1986), Chap. 9.

[9] R. C. Tolman, *The Principles of Statistical Mechanics* (Oxford University Press, London, 1962), p. 626.